BREAST PHANTOM OPTIMIZATION BY A GENETIC ALGORITHM

by

Mosammat Ausnuva Tanbin

A THESIS

Submitted in partial fulfillment of the requirements for the
degree of Master of Science in Computer Science
in the Division of Physics, Engineering,
Mathematics, and Computer Science
of Delaware State University

DOVER, DELAWARE
May 2020

This thesis is approved by the following members of the Final Oral Review Committee:

Dr. Tomasz G. Smolinski, Committee Chairperson, Division of Physics, Engineering, Mathematics, and Computer Science, Delaware State University
Dr. Gary Holness, Committee Member, Division of Physics, Engineering, Mathematics, and Computer Science
Dr. Fatima Boukari, Committee Member, Division of Physics, Engineering, Mathematics, and Computer Science
Dr. David D. Pokrajac, External Committee Member, The Boeing Company

ACKNOWLEDGEMENTS

This dissertation is the result of the journey of my academic endeavors. I have been accompanied and supported by many extraordinary individuals during this journey. It is my pleasure that I have now the opportunity to express my gratitude to all of them.

First and foremost, I would like to express my deepest gratitude to Dr. Tomasz Smolinski and Dr. David Pokrajac. I am lucky to have encountered these two learned and generous persons as my advisors in two consecutive periods of my thesis work. Their guidance, endless patience, constant support and encouragement enabled me to plan and execute my research work in time. They allowed me the freedom in pursuing my research as I found fit, but at the same time, they knew exactly when to give certain reference or insight that I was lacking. The techniques, which I learned from my graduate coursework in Computational Intelligence with Dr. Smolinski, and in Algorithmics with Dr. Pokrajac, had a direct application to this thesis work. Special thanks to Dr. Smolinski for his patience and time in correcting the drafts. Whatever I say, these words are not sufficient to express my gratitude to him.

A very special thanks to Dr. Gary Holness for his continuous advice and support as our graduate advisor as well as for offering the graduate courses of Machine Learning and Advanced Operating Systems. The knowledge, which I gained from his courses, was very useful for my thesis work. I also thank Dr. Fatima Boukari for offering the graduate courses in Theory of Computing, Data Mining & Visualization, and Pattern Recognition. I am grateful for the valuable discussions that I had with her any time I approached her.

I, of course, give thanks to Abdullah-Al-Zubaer Imran for his important contributions to the field. This thesis is the extension of his work. Without his findings, as well as his support with the methods used in his work, it would have been impossible for me to complete my thesis.

I also thank Dr. Predrag R. Bakic, Dr. Andrew D. Maidment, and the entire Department of Radiology at the University of Pennsylvania, for supporting the development of breast cancer research at Delaware State University, and specifically for spearheading the development of a specialized and optimized C++ software for breast simulation that has been utilized for phantom generation in my thesis work.

I gratefully acknowledge all cooperation and support I received from all other faculty members in Computer and Information Sciences at Delaware State University (DSU). In particular, I must thank Dr. Marwan Rasamny for his generous support in everything a graduate student may need during his or her stay at DSU. My deepest appreciation also goes to Ms. Rozena Hawkins, Ms. Rohina Niamat, and Ms. Jacquelyn Jones, for their outstanding logistical support during my studies at Delaware State University.

I am also grateful to the Optical Science Center for Applied Research (OSCAR), as well as the Delaware IDeA Network of Biomedical Research Excellence (INBRE) at DSU, for providing financial support to conduct my research.

I am also very grateful to my family, and especially to my husband, Dr. Jobayer Hossain, and my two sons Araf Hossain Jahin and Jaraf Hossain Rakin. Without their love, patience, and understanding, my academic endeavors would have been difficult. My husband supported and encouraged me to get through the challenging period in the most positive way.

I pay a deep sense of gratitude to my parents who formed a part of my vision and taught me the nice things that really matter in life. The chain of gratitude would definitely be incomplete if I would forget to thank Almighty for his ever mercy, grace, and blessings on this humble being, without which any achievement of my life would not have been possible. My deepest and sincere gratitude to You.

Breast Phantom Optimization by A Genetic Algorithm

Mosammat Ausnuva Tanbin

Faculty Advisor: Dr. Tomasz G. Smolinski

ABSTRACT

The aim of this work is to provide a simulation framework for the generation of anthropomorphic breast phantoms based on the simulation of breast anatomical structures. Three-dimensional breast software phantoms are an important research tool that can help in developing new imaging techniques and devices for the diagnosis of breast cancer. After skin cancer, breast cancer is the most prevalent cancer in women in the United States. Breast cancer can occur in both men and women, but it is far more common in women. Breast imaging system based screening can reduce the mortality rate of breast cancer by improving early detection. Nevertheless, thousands of women are wrongly diagnosed each year. The improvement of breast imaging is an ongoing research. One of the most difficult aspects of this research is to get the human subject data because of the cost, time, or patient risk of repeated use of ionizing radiation. Software phantoms can be used in virtual clinical trials, which allow for an alternative pre-clinical evaluation.

Three-dimensional breast software phantoms have become an important tool used in a variety of fields, including design and pre-clinical testing of novel medical imaging techniques, X-ray dose assessment, and digital pathology. In these phantoms, elements of breast anatomy are described as a set of geometrical shapes, governed by a maximum aposteriori probability (MAP) classifier for a mixture of three-dimensional Gaussian distributions. The phantom geometry is

fully determined by a set of parameters including the distribution parameters, nominal thickness of the simulated breast ligaments and nominal skin thickness. For each particular set of such parameters, a histogram of simulated breast compartment sizes is compared with the histogram estimated by manual segmentation of reconstructed CT images of a mastectomy specimen corresponding to a healthy breast (the CT images were acquired from the University of Pennsylvania and the comparison was performed at the MEDIS Lab at Delaware State University). The comparison was performed using the Kullback-Leibler divergence (KL), Kolmogorov-Smirnov (KS) distance, and Parameterized Distribution Distance (PDD).

To improve realism of simulated phantoms, in the past, phantom parameters were optimized using an exhaustive search within a discretized parameter space. This was done by creating an experimental design using the lower and upper bounds on the parameters. Since this was based on discretizing a continuous search parameter space, we realized that the optimization could be improved by using the continuous parameter space with the evolutionary optimization algorithm.

In this work, we utilized a genetic algorithm (GA) for the optimization of phantom parameters over the continuous parameter space whose initialization was guided by the best solutions obtained from prior work. The proposed approach works in the following way. In each iteration of the GA, the algorithm provides a set of parameters corresponding to a population of potential phantoms to an open source software provided by Dr. Predrag R. Bakic and Dr. Andrew D. Maidment of the Department of Radiology, the University of Pennsylvania. The software then simulates each phantom. This software then calculates the value of the fitness function (e.g., based on KL or KS distance) for each member of the population. The genetic algorithm uses the fitness function values to produce the next generation of GA.

We have successfully developed a set of phantoms with the highest values of the fitness function obtained during the optimization process, all of which combine realistic anatomy with the flexibility of mathematical modeling. Different types of parameters that affect the simulated phantoms have been analyzed thoroughly in the proposed work. These phantoms can be used effectively in imaging research to develop and upgrade new imaging methods and devices in order to detect and prevent the breast cancer.

TABLE OF CONTENTS

LIST OF FIGURES

LIST OF TABLES

CHAPTER 1: INTRODUCTION

SECTION 1.1: PROBLEM STATEMENT

Cancer is the name given to a collection of related diseases. In all types of cancer, some of the body's cells begin to divide without stopping and spread into surrounding tissues. Cancer can start almost anywhere in the human body. Cancer is made up of trillions of cells. Human cells grow and divide to form new cells as the body needs them. When cells grow old or become damaged, they die, and new cells take their place. When cancer develops, however, this orderly process breaks down. As cells become more and more abnormal, old or damaged cells survive when they should die, and new cells form when they are not needed. Then these extra cells can divide without stopping and may form growths, called tumors, and then they are named after the part of the body where the tumor originates. Malignant tumors spread to distant areas. This process is called metastasis (General Information : CANCER AID & RESEARCH FUND).

About 1 in 8 U.S. women (about 12%) will develop invasive breast cancer over the course of her lifetime. A man's lifetime risk of breast cancer is about 1 in 883. According to the American Cancer Society, in 2020, an estimated 276,480 new cases of invasive breast cancer will be expected to be diagnosed in women, and about 2,620 new cases of invasive breast cancer are expected to be diagnosed in men. About 42,690 women and 520 men in the U.S. are expected to die in 2020 from breast cancer, though death rates have been decreasing since 1989 (ACS, 2020). Besides skin cancer, breast cancer is the most common cancer among women in the USA, although women under 50 have recently been experiencing decreases in breast cancer mortality rates. The key to reduce the high mortality rate of breast cancer is early detection and diagnosis. With the improvement in screening and treatment, death rates have decreased from 1.9% between 1988 and

2011 to 1.3% between 2011 and 2017 (ACS, 2019). These decreases are thought to be the result of treatment advances, earlier detection through screening, and increased awareness (ACS, 2019).

SECTION 1.2: BREAST CANCER DIAGNOSIS

Breast cancer can first manifest itself through such symptoms as lumps, rash, swelling of the skin, or itchy or inverted nipple. After discovery of any of these symptoms or abnormalities of the breast, breast cancer can be confirmed by a test such as mammogram, magnetic resonance imaging (MRI), or ultrasound. A mammogram is an imaging technique that uses low-dose X-ray to generate images of the breast to look for early signs of breast cancer. MRI is another imaging technique that uses high-powered magnetic fields, magnetic field gradients, and radio waves, to create images of the organs of the body. Ultrasound is an imaging technique that sends high-frequency sound waves through the breast and converts them into images. But these techniques have several limitations.

SECTION 1.3: IMPORTANCE AND USEFULNESS OF NEW IMAGING TOOLS

In light of the limitations of current imaging techniques, it is necessary to continue to improve breast cancer imaging tools, to evaluate new techniques, and to compare different methods for cancer detection. The clinical trial is performed when a new future imaging technique is evaluated. Also, the new imaging system needs FDA approval. But these clinical trials are restricted by cost and duration. Thus, preclinical trials, also known as Virtual Clinical Trial (VCT), are used. In the United States and Canada, a total of 49,528 asymptomatic women participated as volunteers in a clinical trial for both digital and film mammography (Maidment, 2014). The duration of the trial was 5 years and the cost was $26 million. A virtual clinical trial could be used as an alternative of such a clinical trial. Figure 1 depicts the components of a

process to simulate breast anatomy. This simulation pipeline was developed at the University of Pennsylvania (Maidment, 2014). A VCT simulates human anatomical structure, image acquisition, image processing, image statistical analysis and model observer (Maidment, 2014).

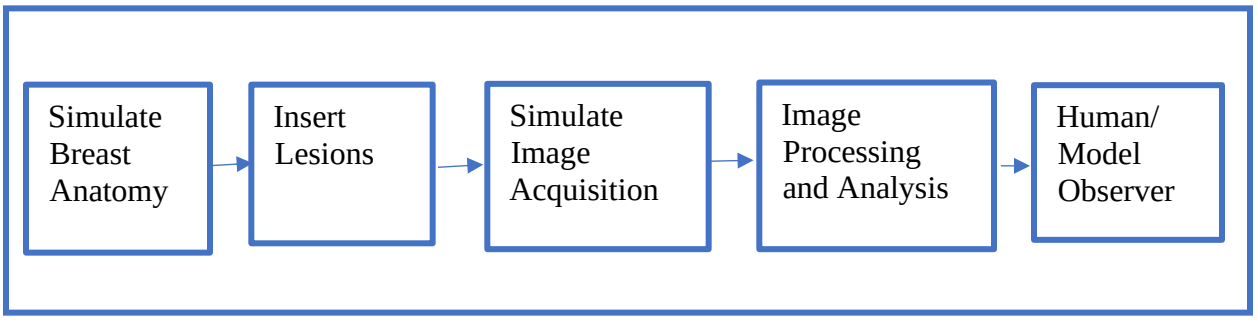

Figure 1. Block diagram of the VCT for simulation of breast anatomy and image statistical analysis (Imran, 2016).

The main objective of a VCT is the simulation of breast phantoms based on the breast anatomical structure. A breast phantom is a breast model that can be used to improve image quality and optimize imaging parameters to detect breast cancer. Such a model typically consists of breast surface, duct system and lobules, connective tissue, Cooper's ligaments, blood vessel systems, as well as skin and breast abnormalities. Breast phantoms can be of different shapes, sizes, and structure. Phantoms can be physical or computerized. Phantoms are utilized to improve the image quality and optimize the imaging parameters that can support the novel imaging techniques. Physical phantoms are limited because they cannot represent different breast sizes, shapes and composition of the breast. It is difficult to simulate patient-specific physical phantoms (Li, Segars, Tourassi, Boone, & Dobbins III, 2009). On the other hand, it is very flexible to simulate any number of computerized phantoms because they are user defined models, and the

user can control the anatomical variations in the breast without additional cost and processing time.

CHAPTER 2: BACKGROUND

Three-dimensional computer simulated phantoms, created based on the structural distribution of the different types of breast tissues and the physical properties of those tissues, can be used for both qualitative and quantitative performance analysis of breast imaging systems. Accordingly, there is an acute need for as realistic simulated phantoms as possible.

SECTION 2.1: BREAST ANATOMICAL STRUCTURE

The female breast mainly consists of a large number of fat cells known as adipose tissue (Neira, Mays, & Hagness., 2017). The breast does not contain any muscle. The amount of fat determines the size of the breast. Compared to the male breast, the female breast is very complex. The adipose tissue spreads from the collarbone to the underarm and also through the middle of the ribcage (National Breast Cancer Foundation). Each of the female breasts also contains 15-20 lobes of glandular tissue. The lobes are divided into smaller lobules that are the glands that produce milk. These lobes and lobules are connected through milk ducts. The milk ducts carry the milk to the nipple. Around the nipple, there is a small circular area known as areola. During nursing, the areola discharges fluid. Breast cancer usually starts to build up inside the breast structure, and is very common in the lobes, lobules, or milk ducts. Figure 2 shows how lobes, lobules, and milk ducts interact with one other in the female breast.

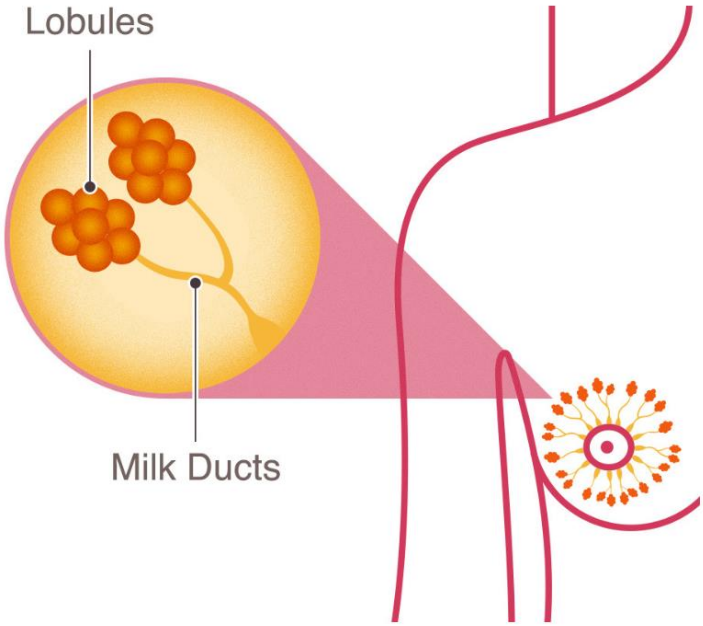

Figure 2. Lobes, Lobules, and Milk Ducts (National Breast Cancer Foundation).

Adipose tissue consists of a group of ligaments, fibrous connective tissue, nerves, lymph vessels, lymph nodes, and blood vessels (National Breast Cancer Foundation). The lymph system composed of a group of lymph vessels and lymph nodes carries disease fighting cells.

Cooper's ligaments are the connective tissue in the breast that maintains the shape and configuration of the breast, and are named Sir Astley Cooper, an English surgeon and anatomist, who first performed qualitative analysis of the distribution and the shape of the adipose tissue compartments in the breast one hundred and seventy years ago (Pacifici). This connective tissue surrounds the lobules and the milk ducts.

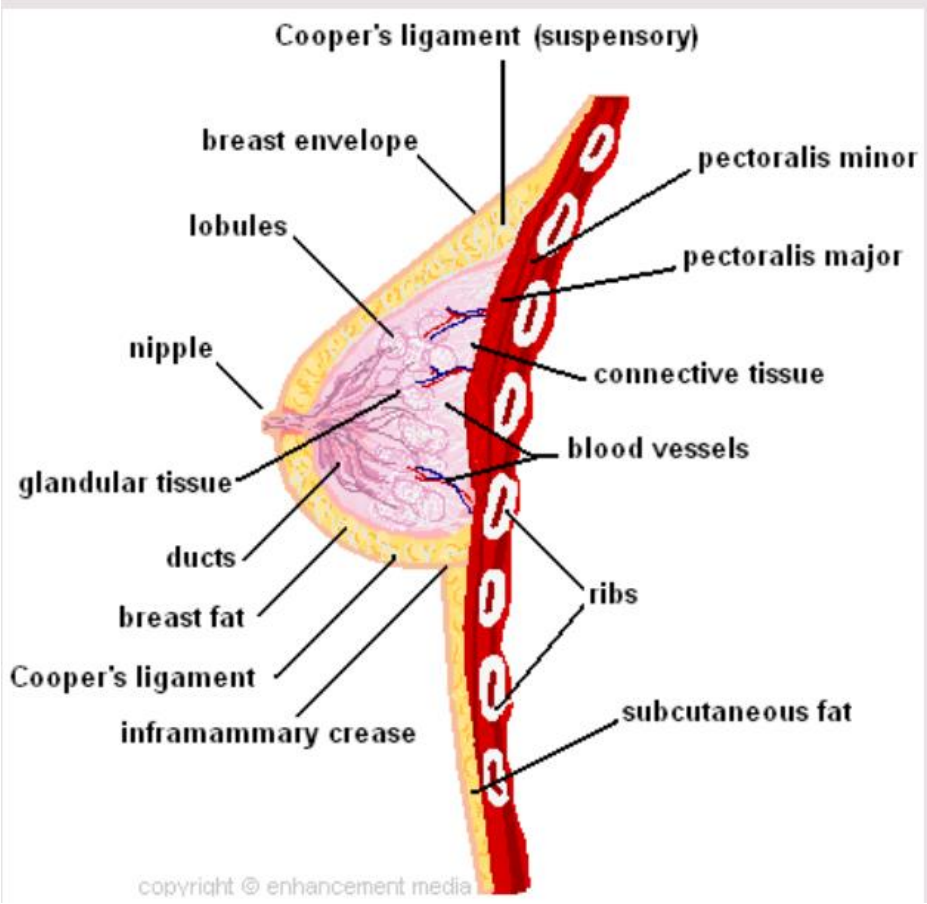

Figure 3. Anatomical structure of a female breast (Breast Anatomy and Structure).

A breast that does not have enough fat tissue will have lots of fibrous or glandular tissues. This type of breast is known as a dense breast. Women with dense breasts have a slightly higher chance of developing breast cancer, as opposed to women with breasts containing more fat tissues. In mammograms, dense tissue and the tumor both look white, so it is hard to distinguish them from each other. On the other hand, the fat tissue appears as black in a mammograph, so it is easier to identify the tumor in less dense breasts. Wolfe (Wolfe, 1976) predicted that there is a high risk of cancer for those women who have parenchymal pattern breasts. Parenchymal pattern defines the pattern of the dense tissues in the breast (Wolfe, 1976). Breast density can be inherited or derived genetically from one's parents or ancestors.

The Breast Imaging Reporting and Database Systems (BIRD) classifies breast density into four categories:

Mostly fatty: When the breast has more fat tissue and less fibrous and glandular tissue that means any tumor can be easily shown in a mammogram.

Scattered density: This type of breast has a bit of fat and has few areas of fibrous and glandular tissue.

Consistent density: This type of breast has more areas of fibrous and glandular tissue that are scattered inside the breast. Accordingly, it would be difficult to identify a small tumor in this type of a breast during mammography.

Extremely dense: This type of breasts has a lot of areas of fibrous and glandular tissue, which makes it more difficult to identify cancer cells in such a mammogram.

SECTION 2.2: BREAST CANCER DIAGNOSIS

Breast cancer can be diagnosed throughout various screening procedures. We can save lives by improving screening tests and treatment techniques. The screening techniques include ionizing radiation techniques and non-ionizing radiation techniques. Non-ionizing radiation does not generate enough energy to separate the molecular bonds and ionize the atoms. On the other hand, ionizing radiation provides enough energy to separate the bonds between molecules and ionize atoms. Ionizing breast imaging techniques such as mammograms, screen-film mammograms, or digital mammograms are most often used for breast cancer detection. Non-ionizing breast imaging techniques include Magnetic Resonance Imaging (MRI), Thermography, Ultrasound, or Optical Imaging.

SECTION 2.2.1: IONIZING BREAST IMAGING TECHNIQUES

Mammography is the most common screening method for breast cancer that gives the visualization of the internal structure of the breast. A German surgeon Albert Salomon, who worked at the Royal Surgical University Clinic in Berlin, is well known for the study of early mastectomies. In 1913, Salomon first observed radiological differences between cancerous and non-cancerous cysts. That is how the history of mammography started (Picard, 1998). But at that time mammography was limited. In 1960, Robert Egan, at M. D. Anderson Hospital and Tumor Institute, in Houston, Texas, defined a reproducible technique that utilized industrial film, which produced excellent breast imaging results for his first 1,000 patients (Bassett & Gold, 1988). During mammography, X-rays of each breast are taken from two different views. One is the Mediolateral Oblique (MLO) view, which is for side-to-side, and the other one is the Craniocaudal (CC) view, which is for top-to-bottom. In addition, breast compression is applied to reduce the thickness of the breast in order to produce better image quality, reduce the X-ray dose, and to better separate tissue (Dustler, et al., 2012).

During the first step of mammography, the technologist will place each of the breasts onto a flat X-ray plate. Then, the compressor will push the breast down to flatten the tissue. This is done for two main reasons: first, compression ensures that the breast will remain still, and second, it prevents the blurring on the X-ray and that helps to produce high quality image. This is uncomfortable, but no one can get hurt during this procedure. The compression only lasts for 20-30 seconds. Then the compression is repeated from different angles and another X-ray is taken. Thus, the radiologist can see the maximum amount of breast tissue as well as the lymph nodes in the breast area close to the underarm. The entire procedure is also repeated for the other breast. The radiologist then carefully examines the mammogram images and provides a report.

Mammography screening requires a small amount of radiation dose and the risk is minimal. The radiation dose is calculated at 4 mGy (milligray) per breast (Heywang-Köbrunner, Hacker, & Sedlacek., 2011). Milligray is the radiation dose unit that is absorbed during mammography. But depending on the breast size and compression, the dose may be different. As the mammographic techniques are improving, the radiation dose is also decreasing.

Digital mammograms are more beneficial for women who are under 50 years because these women tend to have more dense tissues than older women (Herndon, 2016). In digital mammography, X-rays are converted into an electronic picture, which is saved directly onto a computer. That way, the radiologist can see the images right away. When the images on a regular mammogram are not clear, then the computer can help the radiologist better see the images.

Even though mammography is the most effective screening method for early detection of breast cancer, 20-26% of cancers are still missed, and approximately 70% of the biopsies performed are deemed unimportant (Ikejimba, et al., 2017). According to the Food and Drug Administration (FDA), one of the major problems with mammography is that the 3D breast structure is superimposed onto a 2D image plane.

The FDA has approved three types of mammography for breast screening. These are screen-film mammography, digital mammography, and digital breast tomosynthesis mammography.

Screen-film mammography: Screen-film mammography uses X-ray equipment to record the image. X-rays are sent through the breast tissue. Dense tissue, which is connected to cancer, absorbs the X-rays and creates a white region on the film. Here, a breast is X-rayed from center to the side. This type of breast cancer screening is used for women over the age of 40 (Glick &

Ikejimba, 2018). The technician compresses the breast and takes images from different angles for each breast. In the image, breast tissue appears white and opaque, and fatty tissue appears darker and translucent.

Digital mammography: Instead of using X-ray film, in digital mammography, a digital format is used to capture the X-ray images of the breast. This approach also delivers a lower dose of radiation (Glick S. , 2018). Digital mammograms are more accurate for women who have dense breast tissue and are also under 50 years of old (Köşüş, Köşüş, Duran, Simavlı, & Turhan, 2010).

Digital breast tomosynthesis (DBT): Digital breast tomosynthesis is a 3-dimensional (3-D) mammography, which allows tens of angular views of the breast, in a short angular range, with little compression of the breast. This technology constructs 3-D images of the breast by using multiple high-resolution X-rays. DBT is used in combination with a 2-D digital mammography image. Ziedses des Plantes was a pioneer in digital breast tomosynthesis (Plantes, 1971). The FDA has approved digital breast tomosynthesis for breast cancer screening in 2011 (ACS, 2019). Also in 2011, the first commercial DBT system was approved by the FDA to be used in the USA (Karellas, Lo, & Orton, 2008). According to the American Cancer Society, recent studies suggest that digital breast tomosynthesis may reduce false positives, which can improve cancer detection, because the technique slightly reduces breast compression while taking the images, and thus reduces a large amount of overlapped tissues (Sarno, Mettivier, & Russo, 2015). Having said that, DBT is a pseudo tomographic screening procedure, whereas a newer method, the breast Computed Tomography (bCT), is a true tomographic technique. During bCT screening, hundreds of X-ray images of each breast are taken from 360-degree angles. Although bCT provides even less breast compression, bCT is not yet approved by the FDA.

SECTION 2.2.2: NON-IONIZING BREAST IMAGING TECHNIQUES

Non-Ionizing Breast Imaging techniques include: Breast Magnetic Resonance Imaging (MRI) (Saslow, et al., 2007), Thermography, Ultrasound, Automated Breast Ultrasound (ABUS), and Optical Imaging.

Breast Magnetic Resonance Imaging: MRI, also known as Nuclear Magnetic Resonance Imaging, is a scanning technique that uses a powerful magnetic field, radio waves, and a computer, to create detailed images of the breast. Contrast-enhanced breast MRI uses a very high sensitivity tool that can detect cancer even in breasts that are very dense, which would not be easily possible in the mammogram (Bazzocchi, et al., 2006). Breast MRI is not suitable for most patients, however, because it is ten times more expensive than the mammogram, but it may be appropriate for high-risk patients.

Thermography: In thermography, a thermal infrared camera is used to discover and record the temperature changes of the skin. When cancer grows in the cell, enormous blood vessel can be formed in the breast. This areas with a higher skin temperature can be clearly seen in infrared images. Unfortunately, this technique does not provide enough information to detect cancer. It can only mark a person for further investigation.

Ultrasound: The ultrasound procedure uses a transducer that sends high frequency sound waves into the body and receives the responding signal. This is not an uncomfortable procedure. During the procedure, doctor keeps the transducer on the breast. Then, he or she moves the transducer to create clear images of the breast. Ultrasound is safer than other medical imaging procedures. It is also less expensive than other medical imaging options, but its test accuracy relies on the operator's skill and training.

Automated Breast Ultrasound (ABUS): Automated Breast Ultrasound (developed by Siemens Healthcare, U-Systems Inc., and SonoCine) can be used as an alternative to the manually operated ultrasound. ABUS provides high frequency sound waves, which are sent to the target area in the breast to create 3-D volumetric image of the entire breast. These images are useful for women with breasts of high density. ABUS also takes less time for the exam as compared to the traditional Ultrasound.

Optical Imaging: Optical imaging is an imaging technique that uses non-ionizing radiation such as visible, ultraviolet, and infrared light to produce images without causing any side effects by exciting the electrons. The technique provides light propagation inside the tissue components to estimate the optical properties. The optical imaging devices passes on light in the breast in the near-infrared range (NIR) which is up to several centimeters deep. Depending on the tissue components, the light is then absorbed and spread. Different tissue components have different absorbing and spreading characteristics. The detectors record the reaming light and then advanced computer algorithms regenerate the images.

SECTION 2.3: ANTHROPOMORPHIC BREAST PHANTOMS

In the field of medical imaging, a phantom is a specially designed object that is scanned or imaged to evaluate, analyze, and tune the performance of imaging devices in a similar manner to how human tissues and organs would act in that specific imaging modality. An anthropomorphic breast phantom is a three-dimensional (3D) computerized model which simulates breast tissue. A phantom can be used for image analysis or preclinical testing for early breast cancer screening. Computerized breast phantoms can be created using two different approaches: the mathematical approach and the voxelized approach (Li, Segars, Tourassi, Boone, & Dobbins III, 2009). Mathematical phantoms are developed based on varying the composition

of the breast and the voxelized phantoms are developed based on actual clinical imaging data. Mathematical phantoms are more flexible compared to voxelized phantoms, but their images are qualitatively unrealistic (Imran, 2016). The voxelized approach is more realistic than mathematical approach but less flexible because of the difficulty in collecting human subject data that involve more cost, time, and patient risk. There are also approaches that combine these two methods to generate breast phantoms with optimum level of flexibility and realism by selecting the parameters for phantom generation based on empirical data.

SECTION 2.4: PRIOR WORK

The Medical Imaging and Simulation (MEDIS) Lab at Delaware State University (DSU) and the X-ray Physics Lab at the University of Pennsylvania (UPenn) developed software for generating anthropomorphic breast phantoms using a mathematical approach. The phantoms generated by the software are known as the DSU/Penn phantoms (Imran, 2016). DSU/Pen phantoms were generated through the simulation of adipose tissue, fibro glandular tissue, Cooper's ligaments and skin (Imran, 2016). The characteristics of these phantoms were: optimized generation of phantoms, partial volume simulation, insertion of microcalcification automatically, and reduction in the dents, which are a dimpling of the breast tissue. The anthropomorphic phantoms were developed based on an octree recursive partitioning algorithm (Pokrajac, Maidment, & Bakic, 2011) & (Pokrajac, Maidment, & Bakic, 2012). An octree is a tree in which each inner node has exactly eight children. Each octree node was labeled according to a material, such as skin, ligament, fat or dense tissue (Imran, 2016). The phantom outline was characterized by the simulated skin and chest wall. Cooper's ligaments separated the simulated compartments. The octree based recursive partitioning algorithm simulated phantoms with voxel size of up to 25 μm.

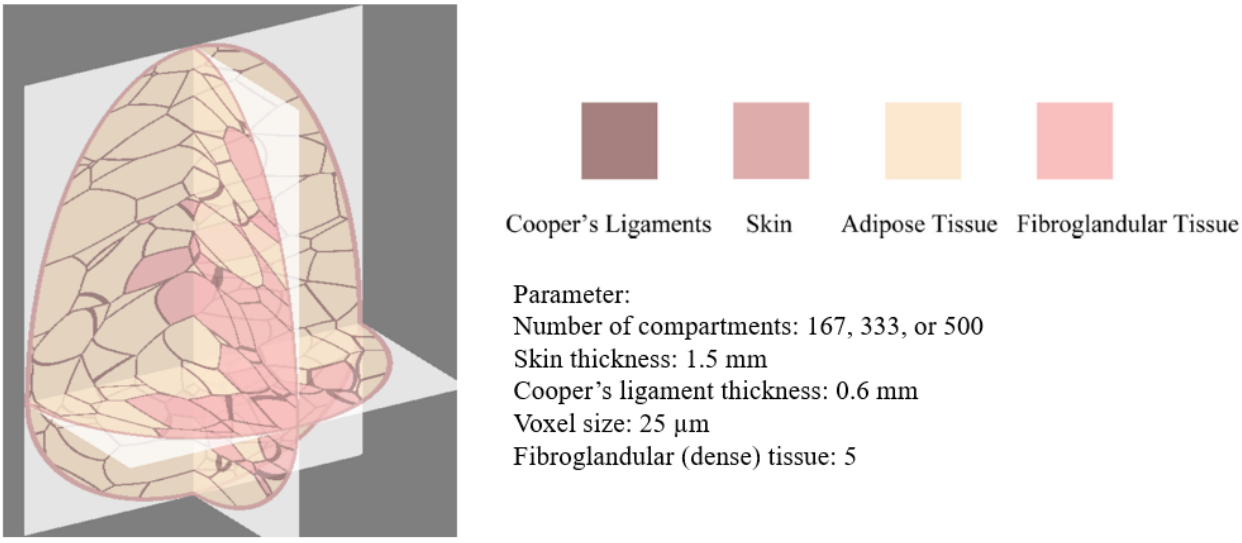

Figure 4. Cross-sections of a 450 cm3 phantom with voxel size 25 µm (Pokrajac, Maidment, & Bakic, 2011).

Breast phantoms can be used in many imaging techniques such as tomosynthesis, CT, dual-energy mammography, ultrasound and dynamic contrast enhanced breast MRI to optimize the imaging procedure.

The work in this thesis is an extension of the work done by Abdullah-Al-Zubaer Imran in 2016 for his master's thesis. In his work, Imran analyzed CT images of a mastectomy specimen, which were collected from the University of Pennsylvania, and the segmentation of the adipose compartments in the breast. First, the adipose compartments of the CT images of a real specimen were segmented, and then the volume distribution of adipose compartments was measured.

In that previous work, the anthropomorphic breast phantoms were generated by an octree-based recursive partitioning algorithm, as described above. Based on the simulation parameters,

which were voxel size, number of compartments, percentage of dense tissue, shape and orientation of the adipose tissue compartments, 1440 phantoms were simulated. After simulation, the volume distribution of 1440 phantoms adipose tissue compartments were calculated and the distances between the software-generated phantoms and the mastectomy CT images were measured. By using different distance measures, the phantoms that were closest to the mastectomy specimen, in size distributional sense, were selected. The Kolmogorov-Smirnov (KS) distance (Massey Jr, 1951), Kullback-Leibler (KL) divergence distance, and Parameterized Distribution Distance measures, were used for the comparison. A multilevel analysis of variance (ANOVAN) of the distance measurements was used to estimate the effect of simulation parameters on the distribution of compartment volumes.

Dr. Pokrajac, Dr. Maidment, and Dr. Bakic published a paper titled "A Method for Fast Generation of High-Resolution Software Breast Phantoms" (Pokrajac, Maidment, & Bakic, 2011), in which they described a method that achieved faster generation of phantoms with small voxel size. The authors compared phantoms simulated with different voxel sizes. Their new breast anatomy simulation improved the simulation time and simulated image quality.

Another article related to this thesis work, "A three-dimensional time domain microwave imaging method for breast cancer detection by using evolutionary algorithm," was published by M. Donelli, et al. in 2011 (Donelli, Craddock, Gibbins, & Sarafianou, 2011). In that paper, the authors presented a novel microwave method that could be used for cancer detection. Using an evolutionary algorithm, they minimized the cost function. Based on the magnetic resonance images (MRIs), they selected three-dimensional simulated breast model. Their method was able to reconstruct the properties of a tumor-like insertion with high accuracy.

In this thesis work, a genetic algorithm (GA) was used to simulate realistic breast phantoms. The details of this implementation are provided in the next chapter.

Genetic algorithms are an optimization paradigm based on biological evolution. In 2016, Aalaei Shokoufeh, et al., used genetic algorithm-based technique for feature selection for breast cancer diagnosis (Aalaei, Shahraki, Rowhanimanesh, & Eslami, 2016). Feature selection is a data pre-processing technique that can identify inappropriate features and remove them to enhance the classification accuracy.

In 1994, James C. Bean utilized genetic algorithms that successfully resolved a range for sequencing and optimization problems (Bean, 1994). The problems were multiple scheduling, resource allocation, and quadratic assignment problem.

Chakir Tajani, et al., used a genetic algorithm to solve the asymmetric traveling salesman problem. In their experiment, instead of using mutation operator, they proposed a new standard genetic algorithm operator, immigration, to maintain the diversity. Immigration and mutation are two different types of genetic algorithm operators. They are both designed to maintain the genetic diversity from one generation to the next generation. By using the immigration operator, entire individuals are generated randomly, whereas the mutation operator randomly mutates one or more gene values in a single individual. Experimental results have shown that the new immigration operator enhanced the performance of GAs on the traveling salesman problem (TSP). Many algorithms have been developed to find out the optimal solution for TSP problem, but genetic algorithm-based search solutions have been especially popular (Khan, Khan, Inayatullah, & Nizami, 2009).

A good amount of research utilizing genetic algorithms for cancer diagnosis can be found in the literature, but not in the area of automatic generation of breast phantoms.

CHAPTER 3: METHODOLOGY

SECTION 3.1: OVERVIEW

In this research, a genetic algorithm-based search technique was utilized to minimize the distance between the simulated phantoms and the real breast (CT images of a mastectomy specimen which will be described below) in order to develop realistic phantoms. Anthropomorphic breast phantoms were generated using some predefined parameters. The input parameters were skin thickness, voxel size, number of compartments, ligament thickness, breast size, percent of dense tissue, combination of speeds, and a random seed generator (Imran, 2016).

The simulation parameters can be varied to generate real phantoms. After simulation, the phantoms are compared with the real clinical image data. For this purpose, the adipose tissue compartment volumes of the clinical image data are required to be estimated. In previous work, the volumetric segmentation of adipose tissues compartment in 3D CT breast images of a mastectomy specimen was performed and analyzed (Imran, 2016). Then, the volumes of the segmented adipose tissues compartments were calculated.

SECTION 3.1.1: ANTHROPOMORPHIC BREAST PHANTOM SIMULATION

To simulate the phantoms, a custom-made simulation software was utilized. The software, called "BPS," was written in C++ (Pokrajac, Maidment, & Bakic, 2011) & (Pokrajac, Maidment, & Bakic, 2012). The phantoms ware generated by replicating the real breast anatomy such as breast skin, air, adipose tissues compartments, Cooper's ligaments, and fibro-glandular tissues (Imran, 2016). The simulator was executed from the command line, with a list of predetermined input parameters. Some of the parameters were kept constant, and others were allowed to vary. The simulation parameters are given below:

Parameter Category	Parameter	Representation
Constant	Voxel size	d
	Breast size	x, y, z1, z2
Nonconstant	Skin Thickness	skin
	Ligament Thickness	t
	Percentage of Dense Tissue	DPercent
	Number of Compartments	c
	Shape Parameters	Speeds
	Random Seed Generator	Srand

Table 1. Parameters for generating breast phantoms (Pokrajac, Maidment, & Bakic, 2012).

The voxel size and the breast size were kept constant and predefined. Other parameters were varied within a range determined by an upper bound and a lower bound.

Breast Size Parameter	Definition
x	In the uncompressed breast, distance between chest and nipple
y	Half of the lateral dimension of the uncompressed breast
Z1	In the uncompressed breast, the vertical distance between top and nipple
Z2	In the uncompressed breast, the vertical distance between nipple and bottom.

Table 2. Definition of breast size parameters (Pokrajac, Maidment, & Bakic, 2012).

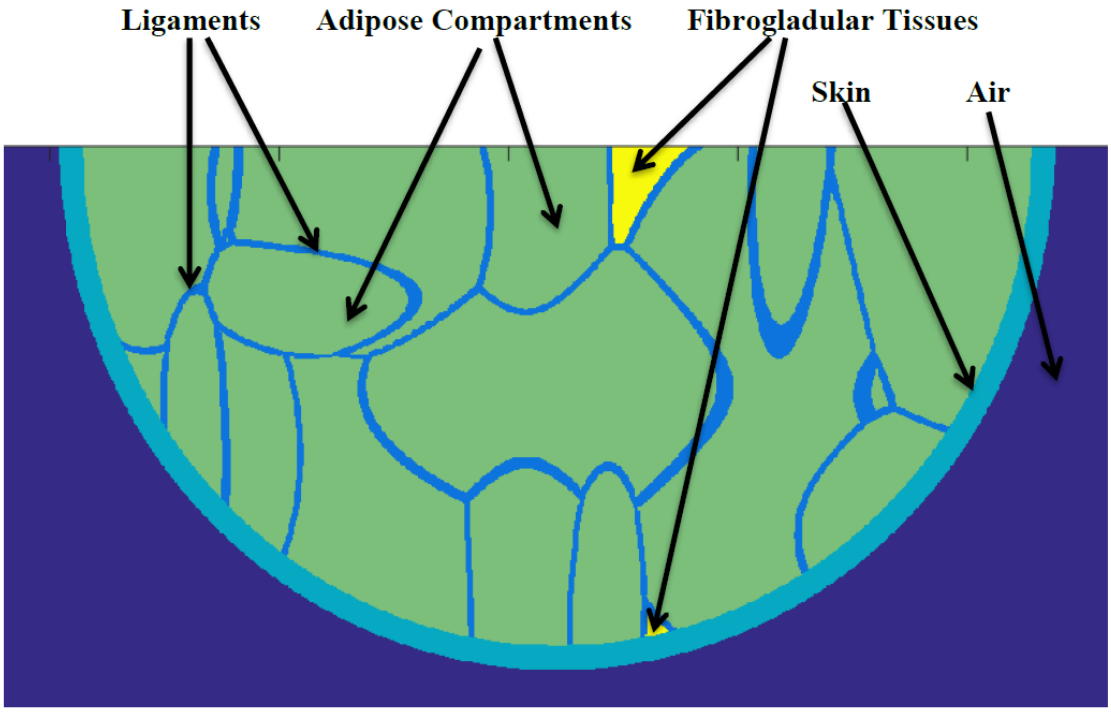

Figure 5. Different components of a simulated breast phantom (Imran, 2016).

After simulating an anthropomorphic breast phantom, the distribution of the adipose tissues compartment volumes was calculated.

The procedure for selecting the optimized parameters for breast phantoms was as follows. After simulating the phantoms, the compartmental volume distribution of each phantom was compared with the CT volume distribution. For this comparison, three different types of measures were used: Kolmogrov-Smirnov distance, Kullback-Leibler divergence, and Parameterized Distribution distance. Since our goal was to minimize the distance, if the distance is very low, the phantom is very close to the real breast. These measures helped us to decide on the realistic phantoms and their parameters.

SECTION 3.2: OVERVIEW OF GENETIC ALGORITHMS

A genetic algorithm (GA) is an optimization technique based on biological evolution. It represents the basic process of the Darwinian theory of natural selection and adaptation. In fact, a GA is in a way a theoretical version of an evolutionary process, and sometimes can also be referred to as an evolutionary algorithm (EA). GAs were proposed in various forms by a number of researchers, but one of the most popular versions was introduced by J. Holland in 1975. In the standard GA, potential solutions to the optimization problem at hand are called individuals or chromosomes. A genetic algorithm operates on a set of such individuals/chromosomes, which make up a population (Grefenstette, 1992). The individuals are encoded into a string of binary bits, real numbers, or characters. Each unit of an individual is known as a gene. The place where the gene is in the chromosome is known as locus.

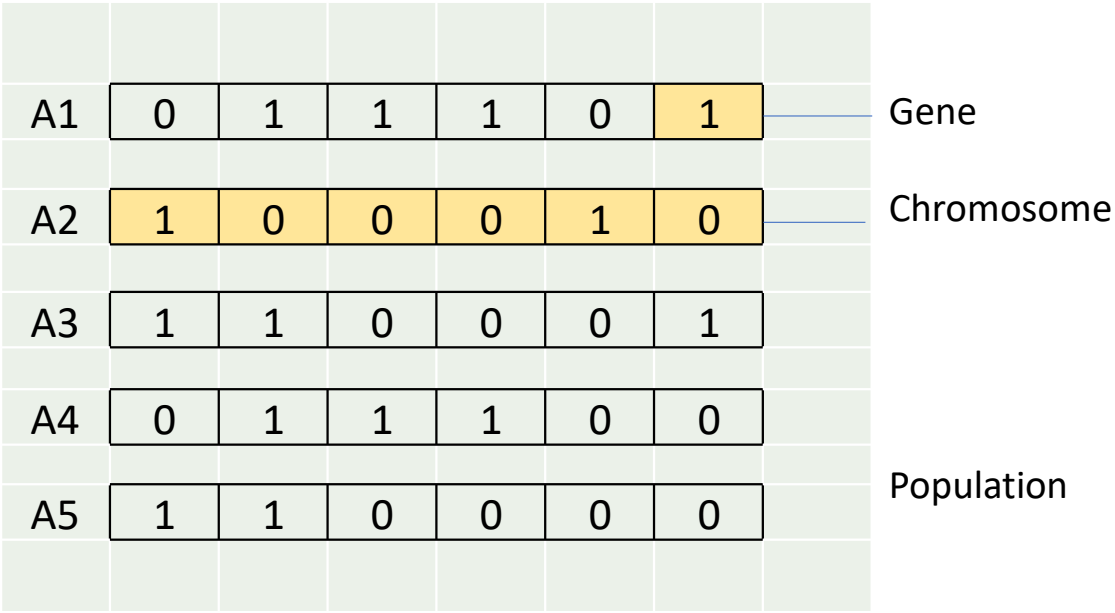

Figure 6. A chromosomal representation in a GA.

Each individual representing a potential solution to the problem at hand is evaluated by a fitness function that measures how good that solution is with respect to that problem. The fitness function is sometimes also called an objective function. In the terminology of GAs, each iteration in the search for the optimal solution is called a generation. At the end of each generation, the fittest individuals are adapted and selected for the next generation.

Typically, a genetic algorithm will consist of the following components:

- Population size represents the number of individuals or chromosomes in a population. If the population size is large, then there will be a better possibility to arrive at the optimal solution quicker (or in fewer number of generations).
- Objective (fitness) function is used to calculate the fitness value of each individual. The fitness value represents how "fit" or how "good" the solution is with respect to the actual

problem. In other words, the better the fitness value, the better the solution in the search space.

- Encoding determines how genes will be represented. There are several possibilities of encoding:

  - *Binary encoding*: The chromosome can be represented as a binary string (0 or 1).

Chromosome 1	0	1	1	1	0	1
Chromosome 2	1	0	0	0	1	0

  - *Value encoding*: The chromosome can be represented as a string of some values. Those values can be numbers, real numbers, or characters.

Chromosome 1	1.76	2.78	8.98	4.78	3.24	4.67
Chromosome 2	AB	SS	BB	LL	LO	KL

- Elitism implies that a number of the best chromosomes should be preserved unaffected for the next generation. For example, if the population size is 10 and the elitism rate is 20%, then the top 2 fittest individuals from the current generation will be transferred to the next generation.

- Crossover is a recombination process, in which highly fitting chromosomes will be selected as parents to generate offspring by exchanging their genetic material. There are different types of crossover:

  - *Single point crossover*: In this crossover, one single crossover point is selected randomly, and then two parents exchange their genetic information at the right side of that point to produce new offspring.

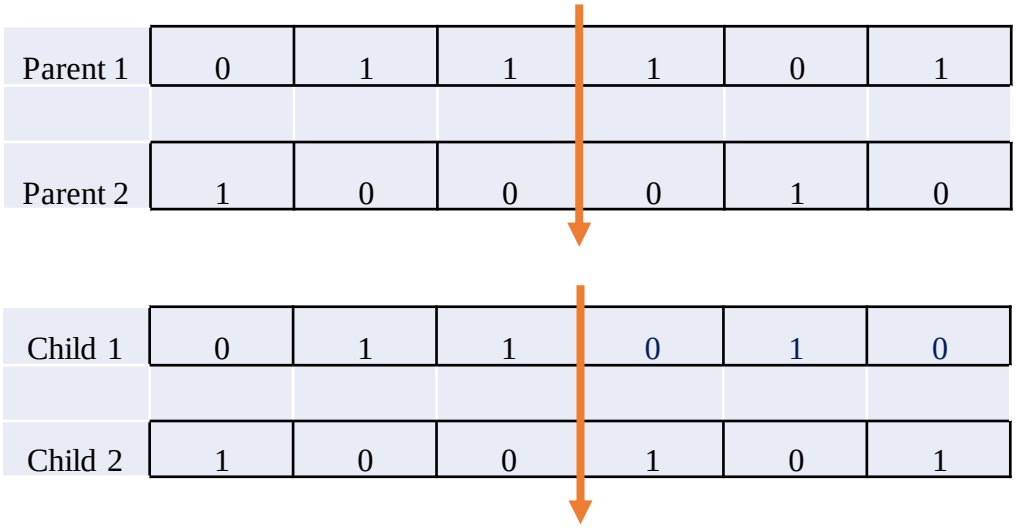

  - *Multi point crossover*: In this crossover, multiple crossover points are selected randomly and then the two parents swap their genetic information among the crossover points to produce new offspring.

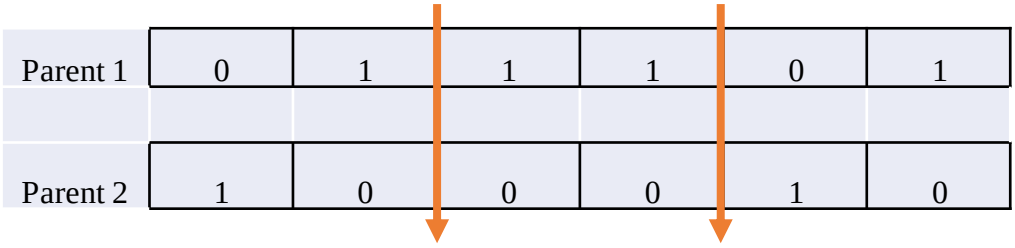

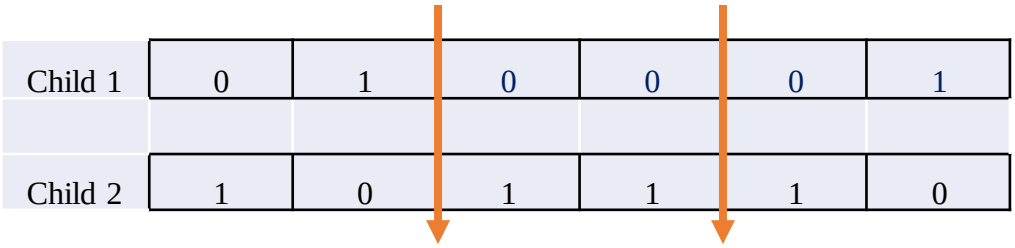

- *Uniform crossover*: In this crossover, each bit of the parents' chromosomes is chosen in proportion to the parents' fitness values. In essence, it is just a toss of a biased coin for each of the parents to decide which parent's gene will be used to generate the new offspring. Each new offspring can inherit the common genes from both parents and at the same time, it can also receive different genes from both parents. For example, in a minimization problem, if parent 1 has the fitness value of 0.25, and parent 2 has the fitness value of 0.15, parent 2 has a higher probability to be selected to produce a new offspring.

							fval	weight
Parent 1	0.75	0.8	10	5	267		0.25	0.375
Parent 2	0.6	0.1	15	1 .	300		0.15	0.625
Biased coin toss	H	T	T	T	H			

Crossed child	0.75	0.1	15	1	267

In some cases, because the crossover points are selected randomly in those two approaches, single or multipoint crossover may be impracticable, as they may have a low probability to select genes from fit chromosomes.

- Immigration is another kind of genetic algorithm operator. By using the immigration operator, the individuals are generated randomly by replacing a portion of the current population from the same allotment in the original population. This approach is very simple (Tinós & Yang., 2007). The random immigration operator gives more diversity in the population. If the fitness value of the local optimum of the population is much higher than all the fitness values of the global search space, that means that the new random individuals have very low survival probability.
- Stopping criteria determine when the algorithm will end. In order to minimize (or maximize) the distance between the true and the target value, a genetic algorithm can iterate through a number of generations. In practice, the number of generations must be explicitly limited.

In summary, a genetic algorithm may work in the following way:

- First, it initializes a random population.
- Then, it calculates the fitness value of each member of the population.
- Then, it selects the members called parents using the roulette wheel selection. Using the parents' chromosomes, the offspring chromosomes are generated by applying the uniform crossover.
- In addition, individuals which have the higher fitness value will be passed for the next generation using elitism.
- The immigration operator can replace a portion of the current population by generating individuals randomly.

- The (crossed over) offspring, elite children, and immigrants, will replace the current population to form a new population for the next generation.
- The GA will stop when it meets one of the given stopping criteria, such as stall generations, stall time limit, fitness limit, or the maximum number of generations.

SECTION 3.3: PROPOSED ALGORITHM

This algorithm proposed in this thesis first started with initializing a selection of population. The population was selected randomly. Table 3 shows an example encoding of an individual in a population.

Fixed					Variable								
d	x	y	z1	z2	sk	c	t	DP	MnS	MxS	MnR	MxR	SR
.01	6.414	6.414	15.394	6.414	.12	267	.05	5	.01	100	.25	4	5000

Table 3. Encoding of an individual.

d - Voxel size

x, y, z1 & z2 – Breast size

sk – Skin thickness

c - Number of compartments

t - Ligament thickness

DP - Percent of Dense Tissues

MnS - MinSpeed

MxS - MaxSpeed

MnR - MinRatio

MxR - MaxRatio

SR - Random seed generator

The voxel and breast sizes were fixed, and the other parameters values were given upper bound and lower bound, which are shown in Table 5 (next section).

The next step was calculating the fitness value. Since the objective here is to minimize the distances, the lower the fitness value (distance), the better the individual. The next two steps in the algorithm were crossover and immigration. In our experiment, instead of using the traditional single point crossover, we used parameterized uniform crossover (Wang & Uzsoy, 2002).

In uniform crossover, two parents are first selected randomly, then a biased coin toss is applied to each parent's gene to decide which parent would pass its genetic information. In our analysis, we created a random number (that is the same concept as tossing a biased coin) and then compared each of the random numbers with the first parent's weight to decide whether that parent's gene would be considered to produce the offspring. If the random number is less than the first parent's weight, then the first parent's gene will pass. Otherwise, parent 2 will pass its genetic information to generate the new offspring. Uniform crossover lets us to influence the search space more strongly to get a better solution because there is a higher chance of selecting genes for the offspring from parents which have better fitness values (Wang & Uzsoy, 2002).

Instead of using the traditional mutation, in this experiment, we used the immigration operator for diversity because it increased the genetic diversity level of the population by randomly generating new members of the population from the same distribution of the original population (Tinós & Yang., 2007).

Three different types of fitness function were used in this experiment for distance measurement:

1. Kolmogrov-Smirnov (KS) distance: The KS statistic quantifies the maximum distance between the empirical distribution function of the data under study and the cumulative distribution function (CDF) of the reference distribution, or between the CDFs of two datasets. In order to compare the datasets from two samples, we estimate their CDFs. Then, the KS distance is the largest absolute difference between the two empirical CDFs evaluated across sorted data points. The KS distance is distribution-free and symmetric. Its value is greater than or equal to zero. It is equal to zero when two distributions are identical (Marsaglia, Tsang, & Wang, 2003).

2. Kullback-Leibler (KL) divergence: The KL distance measures how one probability distribution is different from a reference probability distribution. Suppose P and Q are two distribution functions of two random variables x and y. Then the KL distance is the mathematical expectation of the logarithmic difference between two probabilities distributions, P and Q, when expectation is taken over the probabilities. The KL distance is always non-negative.

3. Parameterized Distribution Distance (PDD): It is the distance between two compartmental size distributions of mastectomy CT and a phantom. Previously, the distribution parameters from the adipose compartment volume distribution of mastectomy CT and each of the software generated phantoms were calculated (Imran, 2016). The weighted sum of the normalized absolute differences of the parameters was calculated as follows:

D_{am} = Arithmetic mean

D_{gm} = Geometric mean

D_{hm} = Harmonic mean

D_{sd} = Standard deviation

D_{md} = Median value

D_{mo} = Mode element

D_{mx} = Maximum element

D_{mn} = Minimum element

D_{sk} = Skewness

D_{kt} = Kurtosis

Table 4 shows the distribution parameters in the order of priority, and the corresponding weight values are assigned to them (Imran, 2016).

Parameters	Assigned Weights
D_{am}	1
D_{gm}	2
D_{hm}	3
D_{sd}	4
D_{md}	5
D_{mo}	6
D_{mx}	7
D_{mn}	8
D_{sk}	9
D_{kt}	10

Table 4. Distribution parameters and their corresponding weight values (Imran, 2016).

Figure 7 outlines the framework of the proposed method, and the pseudo-code for the genetic algorithm is presented below:

Required parameters: Crossover rate p_c, Elite proportion p_e, and immigration rate p_i

1. Initialize random population P

2. Calculate the fitness value of each individual of the population (f_{val})

3. while (stopping criteria of the GA not satisfied) do:

4. Replace a fraction of the population P by the elite proportion p_e

5. for i ← 1 to number of the population size do:

6. P_{new}.individual(i) ← selection of the population (P,i)

7. end for

8. Elitism (P_{new}, p_e)

9. Crossover (P_{new}, p_c)

10. Immigration (P_{new}, p_i)

11. Generate new population P_{new}

12. P ← P_{new}

13. end while

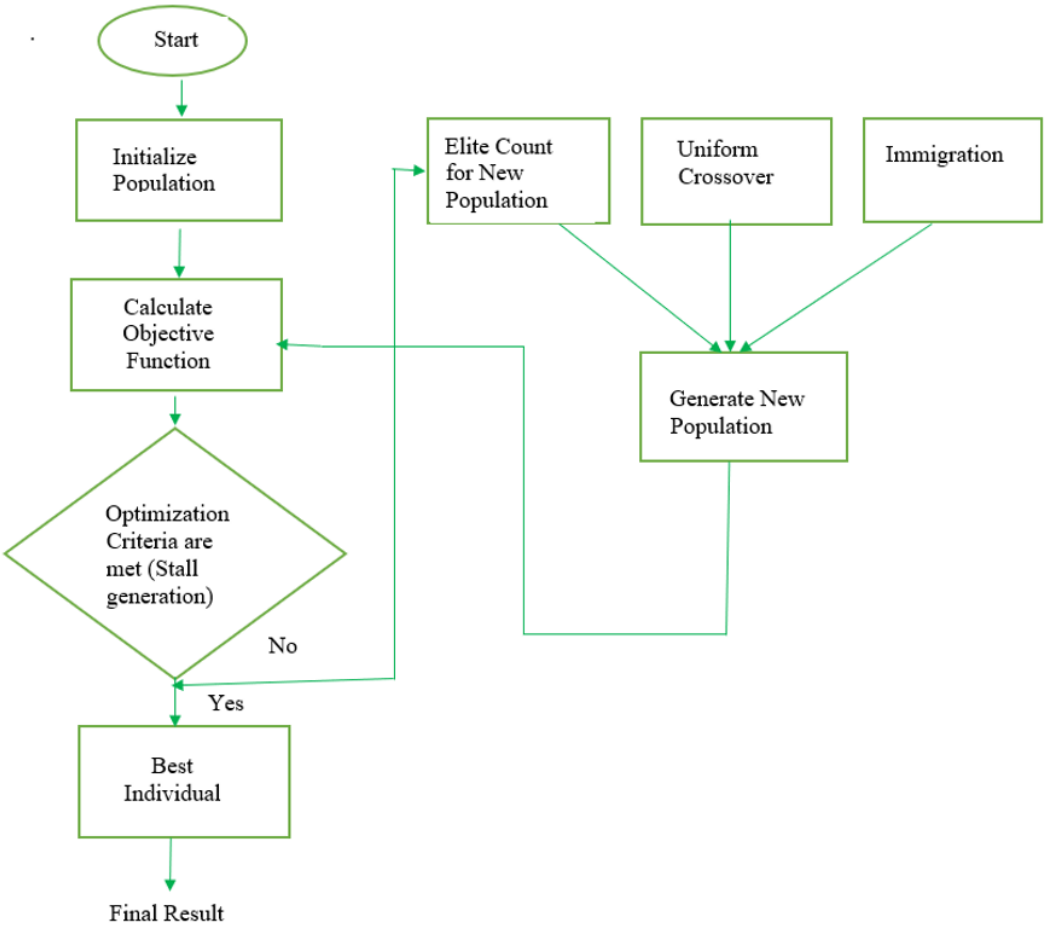

Figure 7. Flow chart of the proposed algorithm.

The main objective of this research was to focus on the simulation of realistic anthropomorphic breast phantoms. By using a genetic algorithm-based search technique to optimize the parameters selection process for generation of realistic phantoms, the approach increases the accuracy level by minimizing the distance between the simulated phantom and a real CT image. For this purpose, the phantom input parameters are varied by the genetic algorithm during the process of generating phantoms. Based on the set of prefixed input parameters, the phantoms are developed.

CHAPTER 4: EXPERIMENTAL SET-UP

SECTION 4.1: GA SET-UP

Our goal was to minimize the fitness values. In our experiments, the population size chosen was 30, and the stall generation was set to 4. 60% of the population was generated by uniform crossover (Wang & Uzsoy, 2002), 20% of the population was generated by immigrating new solutions directly, and 20% of the population was the best chromosomes phantoms from the previous generation (elitism). These parameters were empirically chosen based on preliminary tests, and worked well by balancing the computational time and performance of the GA. Moreover, each genetic algorithm run was replicated three times with different initial random seeds.

The initial population was generated by taking the best solution from prior work (Imran, 2016) as one chromosome, and the rest of the chromosomes were generated randomly for two different measures: the Kolmogorov-Smirnov distance and the Kullback-Leibler divergence. For the third measure, the Parameterized Distribution Distance, two different types of experiments were used. In the first experiment, the initial population was generated by taking the best solution from Imran's work as one chromosome and other chromosomes were generated randomly. In the second experiment, the whole population was generated randomly.

As mentioned earlier, a stall generation of 4 was used as one of the stopping criteria. A stall generation is the number of generations, within the span of which none of the solutions generated by the GA have not improved. Accordingly, here, if there is no improvement in the quality of the breast phantoms in 4 consecutive generations, the stopping criterion is met, and the GA will terminate.

An Intel(R) Xeon(R) machine with CPU 3.50 GHz and memory size 64 GB was used for the experiments described in this thesis. The hardware platform was Ubuntu OS Version 18.04.1. The experiments used Matlab 2018b as the computational engine for implementing the GA. To speed up the GA, multithreading was used on all 4 cores available on the system. The parallelization allowed to simulate 4 phantoms at the same time. Since the population size was 30, it took around 30 minutes to simulate all of the 30 phantoms in a generation. Each of the 30 phantoms was then compressed (by using Imran's code), and its fitness value (KS/KL) was measured. This process of compressing and computing the fitness value for each of the 30 phantoms took approximately another one hour. Accordingly, the total time to run a single generation was around 1.5 hours. The parallelizing reduced the computational time by a factor of 3.5, thus reducing the computational burden of the experiments.

SECTION 4.2: DATA

The dataset used in this experiment was the CT image data of a mastectomy specimen which was provided from the University of Pennsylvania Health System (UPHS) by Dr. Bakic and Dr. Pokrajac. By varying the radiation dose during the CT scan, the quality of the CT images could be improved (Imran, 2016). Previously, the mastectomy was collected from an unidentified contributor. The size of the sample was D-cup and the volume was approximately 907 cm^3 (Imran, 2016). The sample was separated from the body and then it was protected in formalin. The CT imaging process was performed by keeping the sample on an air pocket.

The simulated phantom's volume would be approximately 930 cm^3, which means that the size would be D-cup breast, so that the simulated phantom and the mastectomy CT image would be of the same cup sizes. To simulate the phantoms, fourteen different types of parameters were utilized during the simulation process. Nine of them were varied while the other five were fixed.

Each voxel was predefined to 0.01 cm. The lower bound value of the simulated breast skin thickness was predefined 0.12 cm and the upper bound was set to 0.15 cm. The lower bound and upper bound values for the simulated Cooper's ligament thickness were set to 0.04 cm and 0.06 cm, respectively.

Category	Parameter	Values
Constant	Voxel size (d)	0.01 cm^3
	Breast Size, x	6.414 cm
	Breast Size, y	6.414 cm
	Breast Size, z1	15.394 cm
	Breast Size, z2	6.414 cm
Nonconstant	Skin thickness (skin)	0.12 cm -0.15 cm
	Ligament thickness (t)	0.04 cm -0.06 cm
	Percent of Dense Tissues (DPercent)	0-10
	Number of Adipose Tissue Compartments	167-1000
	MinSpeed (Shape Parameters)	0.01-1
	MaxSpeed (Shape Parameters)	1-100
	MinRatio (Shape Parameters)	0.25-1
	MaxRatio (Shape Parameters)	1-4
	SRand (Random Seed Generator)	1000-10000

Table 5. Simulated phantom parameters, which were predefined by Dr. David D. Pokrajac and Dr. Predrag R. Bakic.

CHAPTER 5: RESULTS

Our goal was to minimize the distance between the simulated phantom and the mastectomy specimen's CT images, and to compare the results obtained using the genetic algorithm with the results of the earlier work (Imran, 2016).

SECTION 5.1: KOLMOGOROV-SMIRNOV DISTANCE BASED EVALUATION OF THE GA

Figure 8 shows the evolution of the Kolmogorov-Smirnov distance as the genetic algorithm progresses. The average and best value of Kolmogorov Smirnov distance in each generation decreases significantly as the genetic algorithm progresses. This happens because genetic operators of crossover and immigration select better sets of parameters to simulate the phantoms as the algorithm progresses. The best distance value remains the same for the last four generations, as the stall generation limit was chosen to be 4.

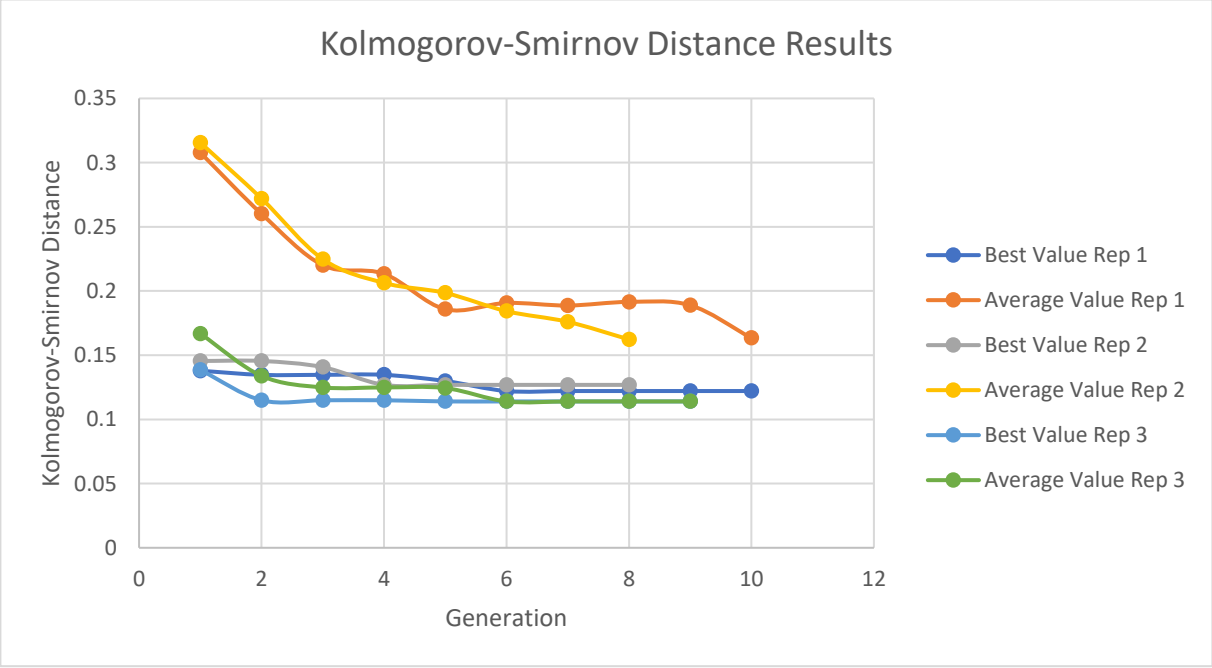

Figure 8. Evolution of the best and average fitness values for the Kolmogorov Smirnov distance for three replications.

A total of 810 phantoms were simulated and evaluated using this distance measure. The best KS value obtained from the GA was 0.1140, which was better than the previously reported value of 0.1457. Table 6 compares the simulation parameters of the best phantom obtained using the GA with the best phantom parameters reported in the previous study. We note that the "Skin thickness," "Number of compartments," "Ligament thickness," and "Percentage of Dense Tissue" parameters are different, and result in a better simulated phantom, with a lower KS distance.

Parameter	Experimental Design Approach for KSD	Genetic Algorithm Approach for KSD
Breast Size (cm3)	930	930
Voxel Size (mm)	0.01	0.01
Skin Thickness (cm)	0.12	0.13
Number of Compartments	1000	789
Ligament Thickness (cm)	0.04	0.07
Percentage of Dense Tissue	5	0
Shape Parameters	0.01 100 1 1	0.01 100 1 1
Random Seed	3000	8635
KS Distance	0.1457	0.114

Table 6. Comparison between the previous approach (Imran, 2016) and the proposed approach for the KSD distance.

SECTION 5.2: KULLBACK-LIEBLER DISTANCE BASED EVALUATION OF THE GA

To evaluate GA performance on minimizing Kullback-Liebler (KL) divergence, we ran the algorithm using KL divergence as the fitness function. Figure 9 shows the evolution of the KL divergence average and best fitness values for each of the three replications of the genetic algorithm.

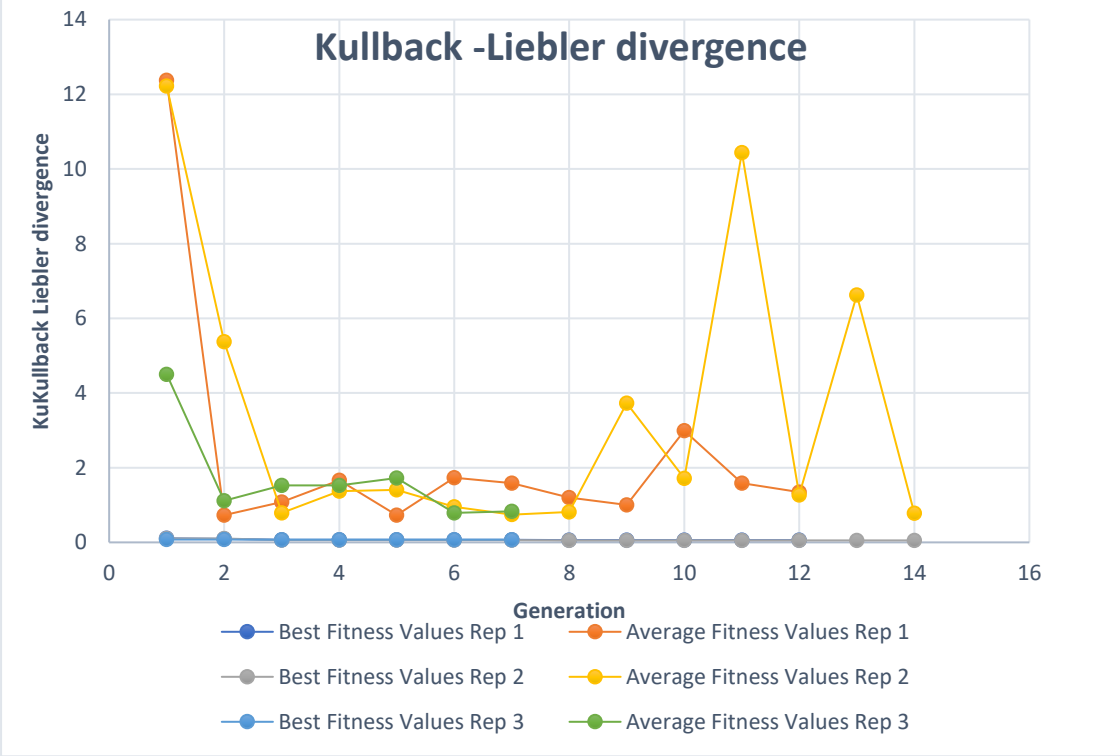

Figure 9. Evolution of the best and average fitness values for the Kullback-Liebler divergence distance for three replications.

We note that there is a significant variation in the average KL divergence as the GA progresses. Since the stall generation number used was 4, the best value remained the same for the last four generations in each of the replications, after which the genetic algorithm stopped.

The GA simulated a total of 990 phantoms, and the best KL distance from the GA was 0.0540, which was better than the previously reported best KL distance value of 0.1108. Table 7 compares the simulation parameters of the best phantom obtained using the GA with the best phantom parameters reported in the previous study. We note that the "Number of compartments," "Ligament thickness," and "Percentage of Dense Tissue" parameters are different and result in a better simulated phantom in terms of its KL divergence value.

Parameter	Experimental Design Approach for KL	Genetic Algorithm Approach for KL
Breast Size (cm3)	930	930
Voxel Size (mm)	0.01	0.01
Skin Thickness (cm)	0.15	0.15
Number of Compartments	500	584
Ligament Thickness (cm)	0.06	0.07
Percentage of Dense Tissue	0	8
Shape Parameters	0.01 100 1 1	0.01 100 1 1
Random Seed	3000	9505
KLD Distance	0.1108	0.054

Table 7. Comparison between the previous approach (Imran, 2016) and the proposed approach for the KL distance.

SECTION 5.3: PARAMETERIZED DISTRIBUTION DISTANCE BASED EVALUATION OF THE GA

To evaluate the GA's performance on minimizing the Parametrized Distribution Distance (PPD), we ran two experiments of the genetic algorithm using PPD as the fitness function.

In the first experiment, the initial population was generated by taking the best solution from prior work as one chromosome, while the other chromosomes were generated randomly. Figure 10 shows the evolution of the PPD average and best values for each of the three replications of the GA seeded with the best solution from prior work.

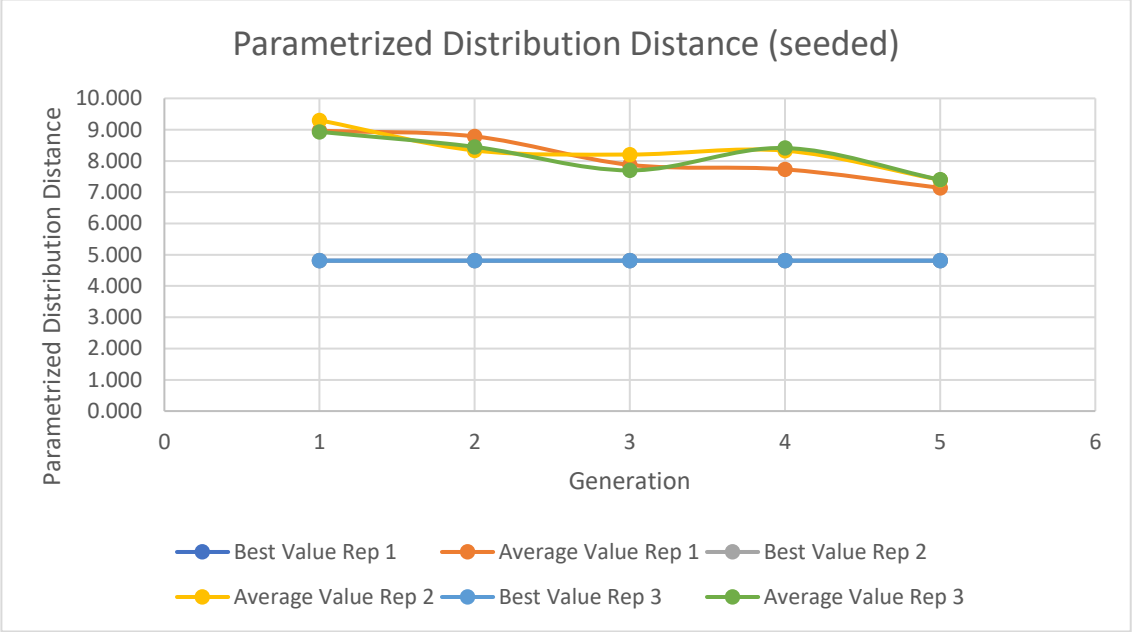

Figure 10. Evolution of the best and average fitness values for the Parameterized Distribution Distance for three replications, experiment 1.

Note that although the average value decreased as the GA progressed, the best value remained the same for all five generations. Each replication stopped after 5 generations as none of the replications could obtain a better value than the one with which they were seeded.

Accordingly, in this case, the GA failed to improve the best value obtained from the prior work (Imran, 2016).

To investigate further, a second experiment was ran, in which the initial population of the GA was generated randomly, without using the best solution from prior work. Figure 11 shows the evolution of the best and average distance values obtained from the GA for each of the three replications.

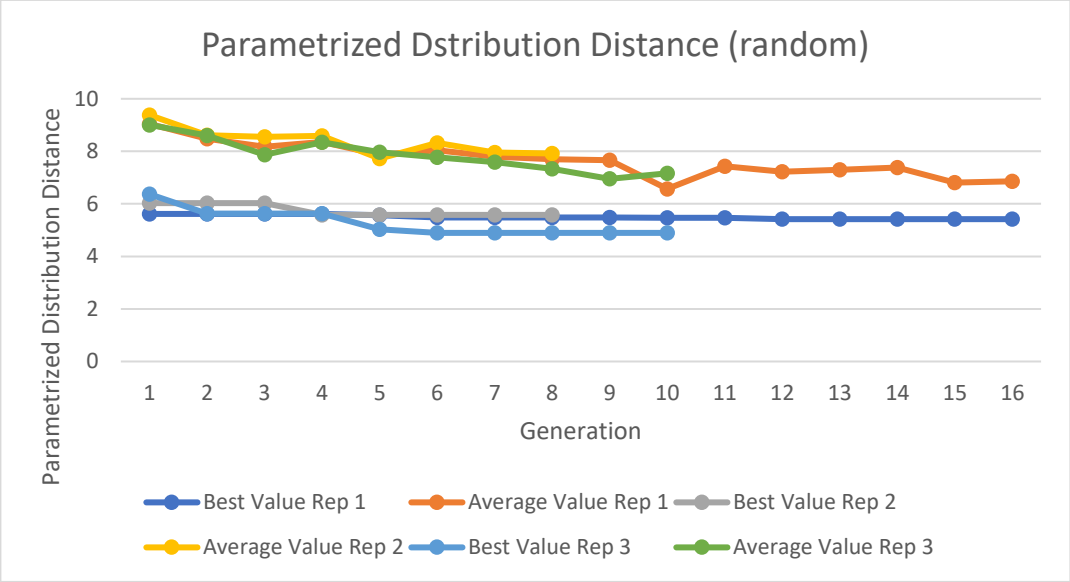

Figure 11. Evolution of the best and average fitness values for the Parameterized Distribution Distance for three replications, experiment 2.

In this case, although the genetic algorithm took longer because it took more generations to stop, it also could not improve upon the best value. The best value obtained using this method was 4.8948 which is worse when compared with the prior best value of 4.809.

This result is perhaps not surprising because PDD was calculated on weighted summary statistics of the simulated and actual phantoms, which makes it more challenging to optimize.

Table 8 shows the simulation parameters obtained for the best phantom simulated using both the prior work and the genetic algorithm (seeded with the best solution). Since both approaches return the same best phantom for PDD, the parameters are also same.

Parameter	Experimental Design Approach for PDD	Genetic Algorithm Approach for PDD
Breast Size(cm3)	930	930
Voxel Size(mm)	0.01	0.01
Skin Thickness(cm)	0.12	0.12
Number of Compartments	1000	1000
Ligament Thickness(cm)	0.04	0.04
Percentage of Dense Tissue	10	10
Shape Parameters	0.01 100 0.25 4	0.01 100 0.25 4
Random Seed	1000	1000
PD Distance	4.809	4.809

Table 8. Comparison between the previous approach (Imran, 2016) and the proposed approach for the Parameterized Distribution Distance.

SECTION 5.4: STATISTICAL ANALYSIS TO IDENTIFY PARAMETERS SIGNIFICANTLY IMPACTING THE FITNESS OF SOLUTIONS

The genetic algorithm described in the previous sections simulated many phantoms in its process of finding increasingly better phantoms. Our secondary objective was to determine which parameters significantly impact the distance measures (KS, KL divergence) in order to help the decision maker with tuning those parameters to simulate more realistic phantoms. Multiple linear

regression was used to analyze the impact of the simulation parameters on the distance measures. Multiple linear regression was calculated for two distance measures: the KS and KL divergence.

Table 9 shows the independent variables used in the multiple regression model, along with their ranges used in the simulation, and Tables 10 and 11 show the results of the analysis for the Kolmogorov-Smirnov Distance and the Kullback-Liebler Distance, respectively.

Parameter	**Value**
Skin Thickness	(0.12-0.15) cm
Number of Compartments	167-1000
Ligament Thickness	(0.04-0.06) cm
Percentage of Dense Tissue	0-10
MinSpeed	0.01-1
MaxSpeed	1-100
MinRatio	0.25-1
MaxRatio	1-4
Random Seed Generator	1000-10000

Table 9. Parameters and ranges of the values used in the regression model.

Variables	Estimated Coefficients	Standard Error	tStat	pValue
Intercept	0.43368	0.042203	10.276	2.3726e-23
Skin Thickness	-0.00093869	0.26934	-0.0034851	0.99722
Number of Compartments	-0.00024116	1.1327e-05	-21.291	**4.8069e-80**
Ligament Thickness	-0.71786	0.16142	-4.4471	**9.9328e-06**
Percentage of Dense Tissue	0.00066477	0.00078453	0.84735	0.39705
MinSpeed	0.0074256	0.0092353	0.80404	0.42161
MaxSpeed	-0.0003481	9.479e-05	-3.6723	**0.00025632**
MinRatio	-0.00074616	0.0096817	-0.077068	0.93859
MaxRatio	0.02849	0.0025186	11.312	**1.2612e-27**
Random Seed Generator	-4.5662e-06	8.9568e07	-5.098	4.2879e-07

Number of observations: 810, Error degree of freedom: 800
Root Mean Squared Error: 0.0599
R-squared: 0.654, Adjusted R-squared 0.65
F-statistic vs. constant model: 168
p-value= 9.98e-178

Table 10. Multiple regression results for the Kolmogorov-Smirnov Distance.

The multiple regression model shown in Table 10 (above) regresses the independent variables on the Kolmogorov-Smirnov Distance. We note that the "Number of compartments," "Ligament thickness," "MaxSpeed," and "MaxRatio" parameters are all statistically significant at 5% level. The coefficients of all these variables are negative implying that the higher the value of these variables, the lower the KS distance value of a phantom. This implies that phantoms with lower KS values can be generated by using higher values of these variables.

The multiple regression output shown in Table 11 (below) regresses the independent variables on the Kullback-Liebler divergence as the response variable. From the regression output, we note that the coefficient of the "Number of compartments" parameter is -0.013343, with the corresponding p-value of 0.00012267. We can say that the number of compartments is significant at the 5% significance level. Since the coefficient for this parameter is negative, the analysis indicates that the larger the number of compartments, the better phantoms, with lower Kullback-Liebler divergence values, can be simulated.

Similarly, the coefficient of the shape parameter (max ratio) has a coefficient of 5.4032 and p-value of 0.0076209. Since this p-value is less than 0.05, the shape parameter is also significant. The positive sign of the coefficient indicates that the lower this max ratio, the better phantoms with lower Kullback-Liebler divergence values can be simulated.

Comparing multiple regression outputs of both KS distance and KL divergence, we note that the number of compartments and max ratio were significant in both. However, the sign for the max ratio was opposite between the two, which makes it difficult to interpret, as max ratio seems to impact KS distance or KL divergence in different ways. The number of compartments variable had negative sign in both outputs, and seemed to be the factor which should be emphasized by the decision maker when trying to simulate breast phantoms.

Variables	Estimated Coefficients	Standard Error	tStat	pValue
Intercept	0	0	NaN	NaN
Skin Thickness	-17.636	41.011	-0.43003	0.66727
Number of Compartments	-0.013343	0.0034602	-3.8562	**0.00012267**
Ligament Thickness	32.852	47.1	0.69749	0.48566
Percentage of Dense Tissue	0.06851	0.14998	0.45678	0.64793
MinSpeed	1.2558	7.7605	0.16182	0.87148
MaxSpeed	0.0059346	0.073919	0.080285	0.93603
MinRatio	3.1839	7.8585	0.40515	0.68545
MaxRatio	5.4032	2.0207	2.674	**0.0076209**
Random Seed Generator	-0.000171	0.00017643	-0.96923	0.33267

Number of observations: 990, Error degree of freedom: 981
Root Mean Squared Error: 14.6
R-squared: 0.135, Adjusted R-squared 0.128
F-statistic vs. constant model: 19.2
p-value= 5.47e-27

Table 11. Multiple regression results for the Kullback-Liebler Distance.

With the KS distance used for fitness evaluation, the regression coefficients for both skin thickness and ligaments thickness were negative. There is no, or a very negligible, effect of skin thickness on minimizing the distance between the simulated and experimental distributions. The estimated regression coefficient (standard error) for skin thickness was -0.00093869 (0.26934),

with a p-value ≈ 0.99722. However, there was a highly significant impact of ligament thickness on this fitness function, with the estimated regression coefficient (standard error) = -0.71786 (0.16142), p-value ≈ 0.0000099.

With the KL distance used for fitness evaluation, the analysis identified a statistically non-significant negative coefficient for the skin thickness parameter (-17.636, p-value ≈ 0.66727), and a statistically non-significant positive coefficient for the ligament thickness parameter (32.852, p-value ≈ 0.48566). Although the raw absolute values of these two estimations are relatively large, the corresponding standardized forms (t-score) are relatively small because of the large variability. Also, the positive coefficient for ligament thickness indicates an increase in the distance between the simulated and experimental distributions for a unit increase in the ligament thickness, which is unexpected, as per the breast anatomical structure, an increase in the ligament thickness is likely to increase the risk of breast malignancy. Therefore, an estimation of a negative coefficient for the ligament thickness would be more realistic for minimizing the distance between the simulated and experimental distributions.

In summary, it appears that the ligament thickness parameter has a biologically feasible impact on minimizing the distance between the simulation and the experimental data using the KS distance. This is not true with respect to the KL distance. These results are consisted with the findings in Imran's original work, in which only the ligament thickness using the KS distance was reported as having a significant effect on the fitness function. This is also consistent with our GA results where we noticed that the average fitness value for the KS distance is more stable than the average fitness value of the KL divergence. Accordingly, the KS distance seems to be a better measure as compared to the KL divergence.

CHAPTER 6: CONCLUSION AND FUTURE WORK

In this research, we used a genetic algorithm to search for simulation parameters that would generate better simulated breast phantoms. The main purpose of this approach was to evaluate the efficiency of genetic algorithms in searching for near-optimal simulation parameters.

By utilizing parametrized uniform crossover, instead of the traditional one-point crossover, the genetic algorithm was able to produce better solutions, as measured by the KS and KL divergence similarity metrics. However, the GA could not generate better solutions for the PDD measure, as PDD turned out to be a difficult function to optimize. This phenomenon could be explained by the fact that PDD is computed by using the summary statistics of the simulated and the actual phantoms, and so does not rely fully on all voxels of the phantoms. Hence, one future research direction could be to evaluate the effectiveness of other meta-heuristics, such as simulated annealing or particle swarm optimization, to search for near-optimal simulation parameters to optimize specifically the PDD function, as in the literature these meta-heuristics are often described as working well for noisy functions similar to PDD.

Using the data generated by the genetic algorithm, we also evaluated the phantom parameters that significantly impacted the simulation. In our experiments, we saw that the number of compartments was a significant variable for anthropomorphic phantom generation as it impacted both the KS and KL divergence measures significantly. However, more carefully designed tests would be needed to substantiate this hypothesis. In future work, this hypothesis should be tested more rigorously, and if determined to be true, it would be interesting to concentrate the efforts on those parameters, which appear to be most significant for phantom generation.

Through the work described in this thesis, we also realized that using KL, KS, and PDD separately as fitness measures in the GA resulted in different phantom parameters, which is consistent with earlier findings by Imran (Imran, 2016). One future direction could be to evaluate trade-offs between these three fitness measures. Based on these findings, a multi-objective genetic algorithm, similar to the single objective genetic algorithm used in this work, could be developed to search for the best set of simulation parameters that optimizes these three objectives simultaneously.

REFERENCES

ACS. (2016). *American Canacer Society: Key statistics about breast cancer?* Atlanta: American Cancer Society.

ACS. (2017). *American Cancer Society: Breast Cancer Facts & Figures 2017-2018.* Atlanta: American Cancer Society.

Bakic, P. R., Albert, M., Brzakovic, D., & Maidment, A. D. (2002). Mammogram synthesis using a 3D simulation. II. Evaluation of synthetic mammogram texture. *Medical physics*, 29(9), 2140-2151.

Bakic, P. R., Maidment, A. D., & Pokrajac, D. D. (2017). Optimization of the simulation parameters for improving realism in anthropomorphic breast phantoms. *Medical Imaging 2017: Physics of Medical Imaging*, 10132.

Baltzer, P. A., Benndorf, M., Dietzel, M., Gajda, M., Runnebaum, I. B., & Kaiser., W. A. (2010). False-positive findings at contrast-enhanced breast MRI: a BI-RADS descriptor study. *American Journal of Roentgenology*, 194(6), 1662-1662.

Bassett, L. W., & Gold, R. H. (1988). The evolution of mammography. *American journal of roentgenology*, 150(3), 493-498.

Bazzocchi, M., Zuiani, C., Panizza, P., Frate, C. D., Soldano, F., Isola, M., *et al*. (2006). Contrast-enhanced breast MRI in patients with suspicious microcalcifications on mammography: results of a multicenter trial. *American Journal of Roentgenology*, 186(6), 1723-1732.

Bean, J. C. (1994). Genetic algorithms and random keys for sequencing and optimization. *ORSA Journal on Computing*, 6(2), 154-160.

Breast Anatomy and Structure. (n.d.). Retrieved from breastlift4you: http://www.breastlift4you.com/breast_anatomy.htm

Contijoch, F., Lynch, J. M., Pokrajac, D. D., Maidment, A. D., & Bakic., P. R. (2012). Shape analysis of simulated breast anatomical structures. *International Society for Optics and Photonics 2012*, 83134J.

Council, N. R. (2005). *Saving women's lives: strategies for improving breast cancer detection and diagnosis.* National Academies Press.

David D Pokrajac, A. D., & Bakic, P. R. (2011). SU-E-I-153: A Method for Fast Generation of High Resolution Software Breast Phantoms. *Medical Physics*, 38(6Part6), 3431-3431.

Donelli, M., Craddock, J., Gibbins, D., & Sarafianou, M. (2011). A three-dimensional time domain microwave imaging method for breast cancer detection based on an evolutionary algorithm. *Progress In Electromagnetics Research*, 18, 179-195.

Dustler, M. I., Brorson, H., Fröjd, P., Mattsson, S., Tingberg, A., Zackrisson, S., & Förnvik, D. (2012). Breast compression in mammography: pressure distribution patterns. *Acta Radiologica*, 53(9), 973-980.

Glick, S. (2018, January 3). *3D Breast Imaging*. Retrieved from https://www.fda.gov/medical-devices/cdrh-research-programs/3d-breast-imaging

Glick, S. J., & Ikejimba, L. C. (2018). Advances in digital and physical anthropomorphic breast phantoms for x-ray imaging. *Medical physics*, 45(10), e870-e885.

Godavarty, A., Rodriguez, S., Jung, Y.-J., & Gonzalez, S. (2015). Optical imaging for breast cancer prescreening. *Breast Cancer: Targets and Therapy*, 7, 193.

Grefenstette, J. J. (1992). Genetic algorithms for changing environments. *PPSN*, *2*, 137-144.

Haus, A. G. (2002). Historical technical developments in mammography. *Technology in cancer research & treatment*, 1(2), 119-126.

Herndon, J. (2016, January 11). *Mammography*. Retrieved from https://www.healthline.com/health/mammography

Heywang-Köbrunner, S. H., Hacker, A., & Sedlacek, S. (2011). Advantages and disadvantages of mammography screening. *Breast care*, 6(3), 199-207.

Ikejimba, L. C., Graff, C. G., Rosenthal, S., Badal, A., Ghammraoui, B., Lo, J. Y., & Glick., S. J. (2017). A novel physical anthropomorphic breast phantom for 2D and 3D x-ray imaging. *Medical physics*, 44(2), 407-416. Retrieved from Medical physics.

Imran, A.-A.-Z. (2016). *Estimation of Breast Anatomical Descriptors from Mastectomy CT Images.* Master's Thesis, Delaware State University.

Imran, A.-A.-Z., Bakic, P. R., Maidment, A. D., & Pokrajac, D. D. (2017). Optimization of the simulation parameters for improving realism in anthropomorphic breast phantoms. *SPIE*, 2, 1-7.

Imrana, A.-A.-Z., Maidment, A. D., Pokrajac, D. D., & Predrag, B. R. (n.d.). Estimation of adipose compartment volumes in CT images of a mastectomy specimen. *SPIE*, 9783, pp. 978320-1.

Karellas, A., Lo, J. Y., & Orton, C. G. (2008). Cone beam x-ray CT will be superior to digital x-ray tomosynthesis in imaging the breast and delineating cancer. *Medical physics*, 35(2), 409-411.

Khan, F. H., Khan, N., Inayatullah, S., & Nizami, S. T. (2009). Solving TSP problem by using genetic algorithm. *International Journal of Basic & Applied Sciences*, 9(10), 79-88.

Köşüş, N., Köşüş, A., Duran, M., Simavlı, S., & Turhan, N. (2010). Comparison of standard mammography with digital mammography and digital infrared thermal imaging for breast cancer screening. *Journal of the Turkish German Gynecological Association*, 11(3), 152.

Kullback, S., & Leibler, R. A. (1951). On information and sufficiency. *The Annals of Mathematical Statistics*, 22(1), 79-86.

Li, C. M., Segars, W. P., Tourassi, G. D., Boone, J. M., & III, J. T. (2009). Methodology for generating a 3D computerized breast phantom from empirical data. *Medical physics*, 36(7), 3122-3131.

Maidment, A. D. (2014). Virtual clinical trials for the assessment of novel breast screening modalities. *International Workshop on Digital Mammography* (pp. 1-8). Cham: Springer.

Männer, R., & Manderick, B. (1992). Parallel problem solving from nature. *The Second Conference on Parallel Problem Solving from Nature*, (pp. 28-30). Brussels, Belgium.

Marsaglia, G., Tsang, W. W., & Wang, J. (2003). Evaluating Kolmogorov's distribution. *Journal of Statistical Software*, 8(18), 1-4.

Massey Jr, F. J. (1951). The Kolmogorov-Smirnov test for goodness of fit. *Journal of the American statistical Association*, 46(253), 68-78.

National Breast Cancer Foundation, I. (n.d.). *Breast Anatomy*. Retrieved from https://www.nationalbreastcancer.org/breast-anatomy

Neira, L. M., Mays, R. O., & Hagness, S. C. (2017). Human breast phantoms: Test beds for the development of microwave diagnostic and therapeutic technologies. *IEEE pulse*, 4, 66-70.

Nichols, H. (2019, Februrary 21). *Tomosynthesis: Breast cancer screening method*. Retrieved from https://www.medicalnewstoday.com/articles/314780.php

Pacifici, S. (n.d.). *Cooper ligament*. Retrieved from https://radiopaedia.org/articles/cooper-ligament?lang=us

Picard, J. D. (1998). History of mammography. *Bulletin de l'Academie nationale de medecine*, 182(8), 1613-1620.

Plantes, B. Z. (1971). Body-section Radiography: History, Image Information, Various Techniques and Results. *Australasian radiology*, 15(1), 57-64.

Pokrajac, D. D., Maidment, A. D., & Bakic, P. R. (2012). Optimized generation of high resolution breast anthropomorphic software phantoms. *Medical physics*, 39(4), 2290-2302.

Predrag R Bakic, M. A. (2002). Mammogram synthesis using a 3D simulation. I. Breast tissue model and image acquisition simulation. *Medical physics*, 29(9), 2131-2139.

Sarno, A., Mettivier, G., & Russo, P. (2015). Dedicated breast computed tomography: basic aspects. *Medical physics*, 42(6Part1), 2786-2804.

Saslow, D., Boetes, C., Burke, W., Harms, S., Leach, M. O., Lehman, C. D., et al. (2007). American Cancer Society guidelines for breast screening with MRI as an adjunct to mammography. *CA: A Cancer Journal for Clinicians*, 57(2), 75-89.

Tajani, C., Abdoun, O., & Lahjouji., A. I. (2017). Genetic algorithm adopting immigration operator to solve the asymmetric traveling salesman problem. *International Journal of Pure and Applied Mathematics*, 115(4), 801-812.

Tinós, R., & Yang, S. (2007). A self-organizing random immigrants genetic algorithm for dynamic optimization problems. *Genetic Programming and Evolvable Machines*, 8(3), 255-286.

Tinós, R., & Yang., S. (2007). A self-organizing random immigrants genetic algorithm for dynamic optimization problems. *Genetic Programming and Evolvable Machines*, 8(3), 255-286.

Wang, C.-S., & Uzsoy, R. (2002). A genetic algorithm to minimize maximum lateness on a batch processing machine. *Computers & Operations Research*, 29(12), 1621-1640.

Wolfe, J. N. (1976). Risk for breast cancer development determined by mammographic parenchymal pattern. *Cancer*, 37(5), 2486-2492.